Astronomical Journal of Azerbaijan, 2022, Vol. 17, No. 2

CIRCUMSTELAR PECULIARITIES OF THE HERBIG AE/BE STARS DERIVED FROM HIGH-RESOLUTION SPECTROSCOPY

M. A. Pogodin [a*], ***N. G. Beskrovnaya*** [a], ***O. V. Kozlova*** [b]

[a] *Central (Pulkovo) Astronomical Observatory, Russian Academy of Sciences, St.Petrsburg, Russia*

[b] *Crimean Astrophysical Observatory, Russian Academy of Sciences, Nauchny, Crimea, Russia*

An overview of the results of spectroscopic observations of the Herbig Ae/Be stars at different observatories starting from 1986 in the framework of the Pulkovo program is presented. The aim of the program is to study structural, kinematical and physical properties of the circumstellar envelopes around bright objects from the catalogue of candidates to the Herbig Ae/Be stars by Thé et al. (1994). As a result, long-term spectroscopic monitoring of 10 Herbig Ae/Be stars have been carried out. Two main groups of the program objects can be distinguished. The first group includes three yearly type (B0–B3) massive star. All of them have been found to be binary systems and demonstrate some unusual inexplicable phenomena. The second group contains B9–A4 stars with signatures of dense outflowing matter on the line-of-sight between the star and the observer. The analysis of their spectroscopic variability allows to investigate structural and kinematical features of their circumstellar envelopes. A special case is the B6e Herbig star HD 259431. There is good reason to believe that this object is surrounded by a magnetosphere, that is in contrary with earlier predictions by other investigators.

Keywords: stars: pre-main sequence – stars: early-type – techniques: spectroscopy

1. INTRODUCTION

Now it is commonly recognized that Herbig Ae/Be stars are young pre-main sequence objects of intermediate mass. They are surrounded by relict accretion disks responsible for their observational features:

* E-mail: mikhailpogodin@mail.ru

a) the far IR excess and b) the emission line spectrum [2–4]. The accretion from the disk onto the star takes place near the equatorial plane, where the disk is situated, and than – through the stellar magnetosphere. A matter outflow can be observed at higher latitudes (a so called wind).Several different scenarios of the envelope/star interaction are considered now. Many properties of these objects are already clarified. Nevertheless, some observed phenomena remain unclear. As a practice shows, long-term spectroscopic monitoring of the program objects on the time scales from hours to years is an effective way to collect information on physical processes taking place in the CS envelopes. We started our observations in 1986 at the Crimean astrophysical observatory with different spectrographs of high resolution ($R \sim 20\,000$). Additionally, we carried our observations at such observatories as ESO (Chile), OAN SPM (Mexico), Kourovka AO (Ural FU) and others. About 2 000 spectra of 10 objects have been obtained during 35 years. Sometimes the spectroscopic programs were followed by photometric and polarimetric observations. In this paper only several the most interesting results are presented. All objects of our investigation were the brightest stars ($V < 9^{\mathrm{m}}$) chosen from the catalogue of candidates to Herbig Ae/Be stars by The et al. [4]. As it was found, two main sub-groups can be distinguished:

1. Early-type Be stars (HD 200775, HD 53376, HD 52721);
2. Ae stars with signatures of dense wind between the star and the observer (AB Aur, HD 163296, HD 36112, HD 31648, HD 37806, HD 190073).

A special case is the Herbig B6e star HD 259431. It was turned out, that the first sub-group of the most massive and early-type objects demonstrate the most puzzling unresolved properties. In this paper we concentrate our attention on the objects from this sub-group.

2. HD 200775

The first object from this sub-group is the bright northern star HD 200775. It is a well-known Herbig B3e star in the reflection nebula NGC 7023. During 16 years we have observed this object at 6 observatories. There were Crimean AO, Ritter AO (USA), OHP (France), Hawaii and McDonald AO (USA), SAO RAS (Northern Caucasus). About 200 high-resolution spectra near $H\alpha$ have been obtained. The results were presented in Beskrovnaya et al. [4], Pogodin et al. [5,6]. The $H\alpha$ in the spectrum of HD 200775 is seen in emission. We confirmed earlier result of Miroshnichenko et al. [7], and found, that different parameters of the line demonstrate a cyclic variability with the period about 3.7 years. So, the EW of the emission profile becomes twice greater in its maximum in comparison with

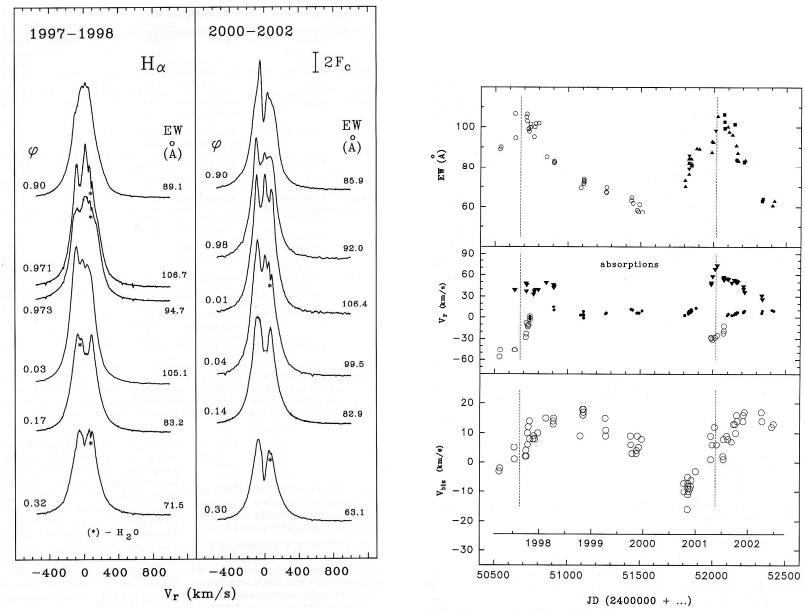

Fig. 1. *Left*: Typical emission $H\alpha$profiles of HD 200775 at different phases of activity (for $P = 1345$ days) during different observing seasons. The zero phase corresponds to maximum of EW. *Right*: Variations of different parameters of the emission $H\alpha$ profile in 1997–2003. *Top* panel: equivalent width (EW); *middle* panel: positions of local absorption components; *bottom* panel: bisector velocity at the normalized intensity level 1.5–2.0 F_c. This parameter corresponding to the velocity of the star was used to obtain the orbital solution for HD 200775 as a binary system.

the minimum (Fig. 1). In the minimum state the profile is double-peaked. But in the maximum it looks as a single profile with a number of local components near the top. The picture of positional variations of these features is rather complex, but it repeats from cycle to cycle. It is remarkable, that the curve of the bisector velocity of the emission profile calculated at the twice the continuum level resembles a curve for radial velocities of components of a binary system. At this level we observe wide emission wings forming in equatorial gaseous disk near the stellar surface. Since the disk is axially symmetric, the bisector velocity corresponds to the velocity of the star itself. We assumed that observed variability of this parameter is a result of binarity of HD 200775. And the temporal curve of this variability can be considered as a radial velocity curve for a component of the binary system surrounded by the gaseous envelope. We derived the orbital solution for the system. The orbital period was determined more correctly. We estimated also the eccentricity and the phase of periastron (Fig. 2). Different symbols on the plot correspond to data from different observatories. Our estimations

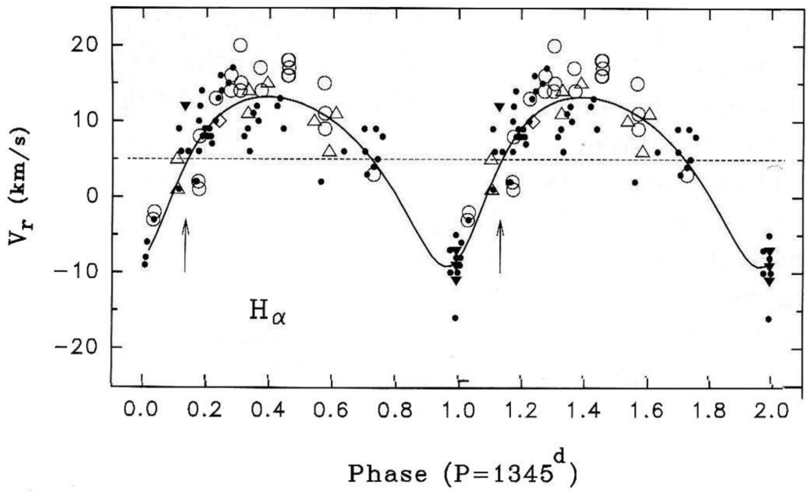

Fig. 2. Orbital solution for HD 200775 on the base of $V_{\rm bis}\,(H\alpha)$ at the 1.5–2.0 F_c level. Different symbols correspond to data obtained at different observatories. The arrows indicate the position of the EW maximum.

were as follows: $P = 1341 \pm 23$ days, $e = 0.29 \pm 0.07$, phase 0 corresponds to periastron. We were carrying out our observations only in $H\alpha$ and could get no information on the second component of the system. But our study was followed by other investigators. Some years later, the orbital solution for both components was obtained by Alecian et al. [8]. The observations were carried out with the spectropolarimeter ESPaDOns of very high resolution and using the LSD (Least Squares Deconvolution) method. They reconstructed orbital velocity curves for both components. It has turned out that they are stars of similar masses. Their determinations of the main orbital parameters were found to be close to our results: $P = 1412 \pm 54$ days, $e = 0.32 \pm 0.06$. They estimated several parameters of both components of the system (A and B), these values were very similar for A and B components, except $V \sin i$ (26 km/s for A and 59 km/s for B). The most recent and exact estimation of the orbital period of the system has been obtained at Kourovka Observatory ($P = 1361.3 \pm 2.2$ days, [9]). Alecian et al. [8] constructed also the bisector velocity curve for the $H\alpha$ emission profile, as it was made earlier by us. It turned out that this curve agreed with the curve for the secondary (B). That means, that only the secondary is surrounded by the gaseous envelope. The second surprising fact: only the primary demonstrates signs of large magnetic field of about 1 kG. The distance between the components is about $200R_*$ in apoastron and $100R_*$ in periastron. When the components A and B draw close together, the envelope of B component becomes excited. To explain what processes take place in the system is a problem of MHD modelling of CS gas.

3. HD 53367

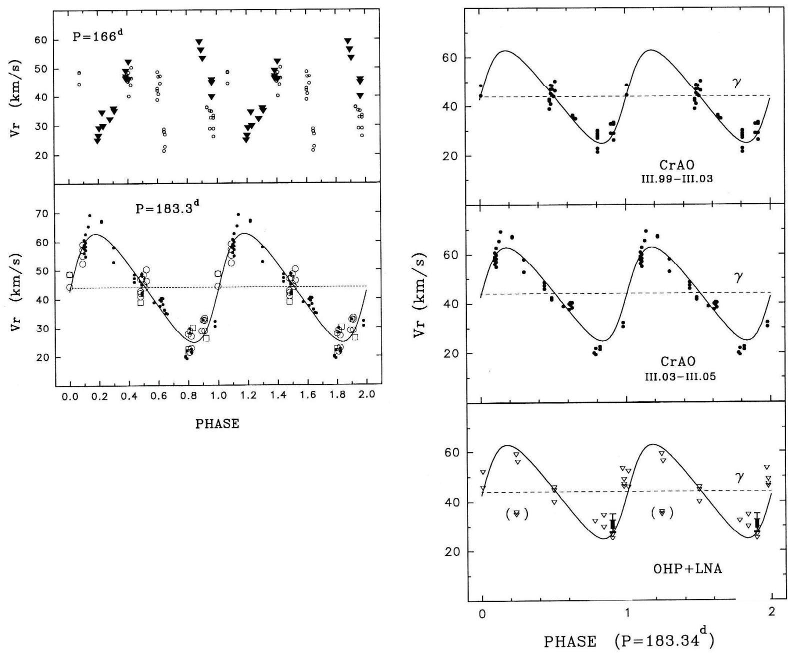

Fig. 3. *Left bottom*: The orbital solution obtained in our investigation. Left top: Our data converted with the period $P = 166$ days, obtained in [17]. Right: Our data obtained in different seasons from 1999 to 2005 fitted by the orbital curve calculated for $P = 183.34$ days.

It is the brightest B0-type PMS object in the extended star formation region CMaR1. The stellar composition of the region was studied in detail by Tjin A Djie et al. [4].

More than 200 $UBVR$ measurements of HD 53367 were collected during 12 years at the Mt. Maidanak Observatory and more recent data were kindly put at our disposal by K.N. Grankin. In addition, spectroscopic observations were carried out at 3 observatories: a) Crimean AO, b) LNA (Brazil), and c) OHP (France). Near 110 high-resolution spectra have been obtained. Results of this program were published in [11].

We have found that HD 53667 is a binary system and derived the orbital solution for this object based on our spectroscopic data using velocities of 2 atmospheric

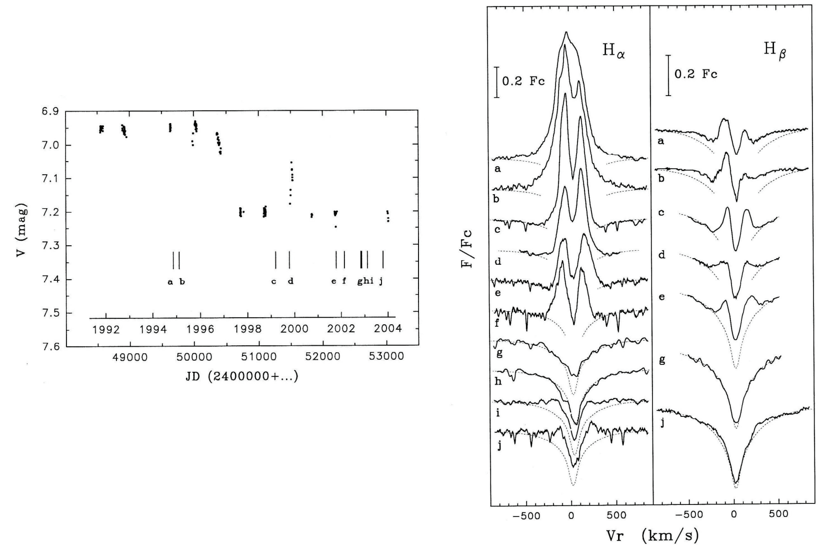

Fig. 4. Left: The V light curve of HD 53365 from 1992 to 2004. Right: The $H\alpha$ and $H\beta$ profile variability in the spectrum of HD 53367 during the dissipation of its gaseous disk-like envelope and the consequent emergence of the new envelope.

lines: OII 6641 and HeI 6678 (Fig. 3, left bottom). We estimated the orbital period $P \sim 183$ days, which is in contrast with the previous estimation by Corporon & Lagrange [17], where $P = 166$ days. We can see that our observations did not confirm their result (Fig. 3, left top). We believe that it is connected with the fact that Corporon & Lagrange in their calculations used velocities of the HeI, which is strongly under CS influence.

Figure 3 (right) illustrates a satisfactory fitting of our data obtained at different seasons and at different observatories by our orbital curve. The secondary component is likely to be a low-mass star, and its spectroscopic signatures are invisible. The photometric study of this object show that it has a peculiar light curve with 2 states of brightness: high and low (Fig. 4, left). The time scale of their change is several years. This variability is likely to be a result of variations of the amount of emitting gas in the envelope. The inference is based on the fact that the object becomes more red in the bright state.

This conclusion is confirmed also by results of our spectroscopy. It turns accidentally out, that the period of our spectroscopy covers the dates of transformation (see symbols in Fig. 4) of the object from high to low photometric state (Fig. 4, *right*). In the high state, the emission Balmer line profiles are wide and large in intensity. Then they become more narrow and less intense. At last the emission disappears completely, and we see only the atmospheric profiles. But some time

later an emission component forms again. It is small in intensity but rather broad. Such picture of profile variations corresponds to the situation, when the gaseous equatorial disk starts its dissipation beginning from the most internal region near the stellar surface, where the velocity of rotation is high. Then it transforms into a remote CS ring with small rotation velocity. And, at last, the envelope dissipates completely.
Then, the CS disk-like envelope reappears again, staring its rising from the stellar surface, where the rotation velocity is high and the emission line has to be broadened. This phenomenon is usual for classical evolved Be stars, but was not observed earlier in PMS Be stars.

4. AE STARS WITH SIGNATURES OF DENSE WIND

The second sub-group of objects of our program includes Herbig Ae stars with signatures of a dense wind in the field between the star and the observer. These objects demonstrate P Cyg-type profiles of spectral lines, with $H\alpha$ as the most prominent emission line. The profiles can look as P CygII (or classical P Cyg) profile with a blue absorption component, P CygIII profile with small emission peak at the blue boundary of the absorption component and as a purely single emission profile (Fig. 5). The profiles , as a rule, demonstrate variability on timescale of days in a form of transformations between these 3 types.

We propose a possible interpretation of this phenomenon. Our assumptions are as follows:

- the equatorial accretion disk is inclined relative to the line-of-sight;
- the wind zone is situated at higher latitudes on both sides of the disk;
- the wind is accelerated by the magnetic centrifuge until certain distance R_m, then it moves with deceleration according to the Keplerian law;
- the wind zone increases in its latitudinal distribution with distance (the wind is flared);
- Three cases of intersection of the wind zone by the line-of-sight can be separated: A, B and C. (Fig. 6, *top*).

In this situation, if the wind zone is wide enough and screens the star at all distances from the star, the classical P Cyg-type profile without additional blue emission maximum (P CygII) is observed (A). If the flared wind starts to screen the star only at some intermediate distance $R > R_m$, the stellar emission at high velocities has to be seen in a form of the blue emission peak (P Cyg III) (B). And,

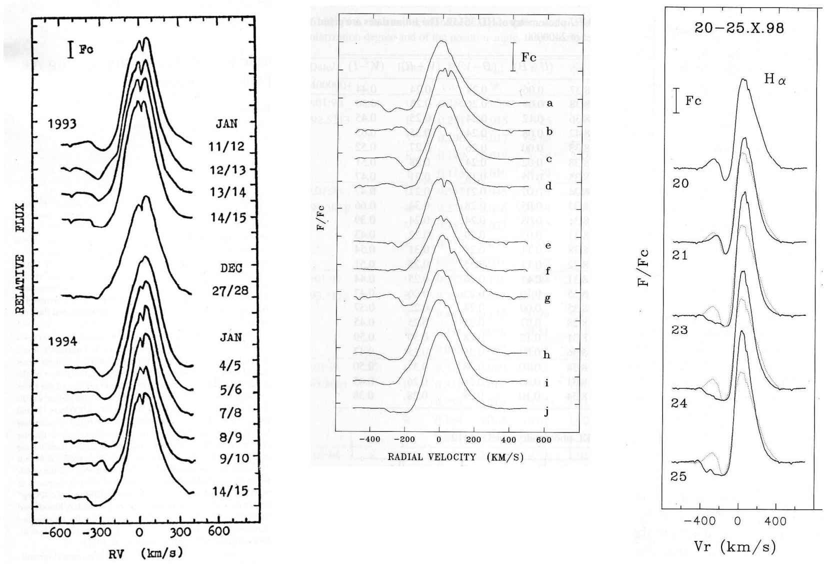

Fig. 5. Typical emission $H\alpha$ profiles in the spectra of AB Aur, HD 36112 and HD 31648 (from left to right) in different observing data. They are taken from Beskrovnaya et al. [4, 6, 9], correspondingly.

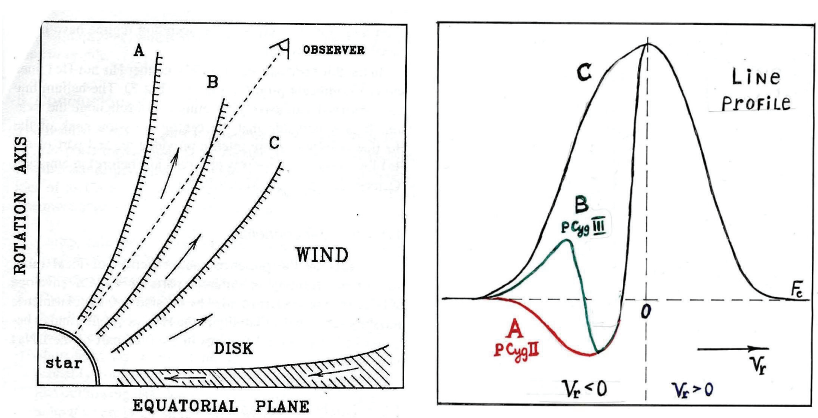

Fig. 6. *Left*: Schematic geometry of the wind zone, and 3 cases (A,B,C) of its intersection by the line-of-sight. Right: The line profiles observed in each of the cases A, B and C. The details are given in the text.

at last, if the wind zone is narrow and does not screen the star at any distances, one can see only a symmetric emission profile without absorption component (C) (Fig. 6, *bottom*).

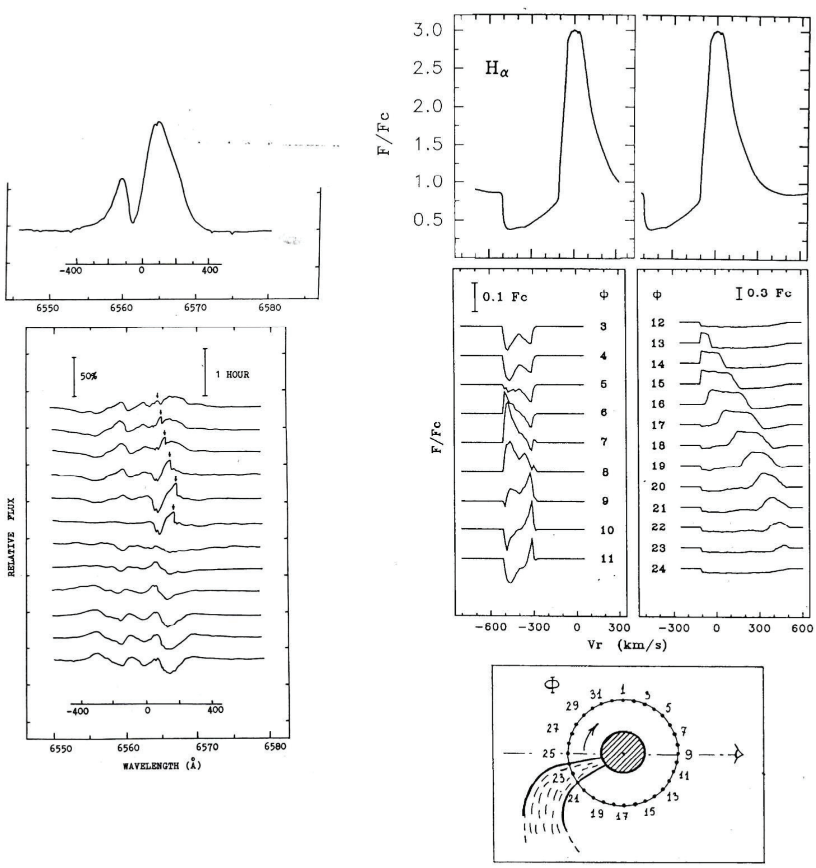

Fig. 7. Left: The nightly mean $H\alpha$ profile observed in the spectrum of HD 163296 on July 26, 1992 [12] and the individual residuals constructed relative the nightly mean profile. The time is directed from top to bottom. Right: The theoretical P Cyg-type profiles and their residuals calculated for different phases of a local stream rotation relative to the line-of-sight. The details are given in the text.

As a result, the observed profile transformation can be explained by a latitudinal re-distribution of the wind zone. The second typical variability of the line profiles in spectra of Herbig Ae stars with signatures of strong wind is appearance of standing waves at the blue part of its P Cyg-type profiles. Figure 7 (*left*) illustrates residual profiles obtained during one night constructed relative to nightly mean and relates to the Herbig Ae star HD 163296 and its $H\alpha$ line. The spectra were obtained at ESO in 1991 [12]. The short-term variability is seen in the residuals in the form of: a) a standing wave in the region of the blue P Cyg-absorption; b) a running wave in the red parts of the emission profile. Similar character of variability is observed in other Herbig Ae/Be stars of such

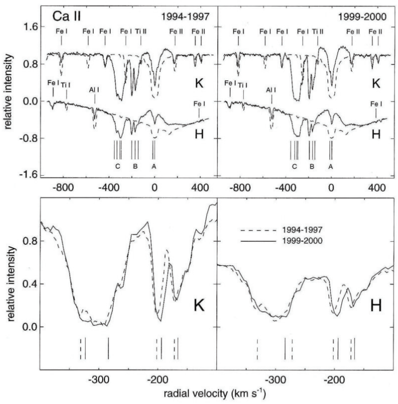

Groups of CS components	OHP (1994–1997)	ESO (1999–2000)	Previous data (1943–1974)
A	0 ± 1	+3 ± 2	+5−−5
	−17 ± 1	−15 ± 2	−12−−15
B	−145 ± 1	−146 ± 1	−143−−155
	−172 ± 1	−166 ± 1	−168−−188
	−202 ± 1	−194 ± 1	−198−−212
	−225 ± 2	−226 ± 2	−227−−237
	−236 ± 1	−238 ± 3	−238−−243
C	−272 ± 2	–	−265−−274
	–	−284 ± 1	
	−294 ± 1	−295 ± 1	different sets
	−305 ± 3	−304 ± 1	of local
	−331 ± 1	−323 ± 2	features between
	−354 ± 2	−358 ± 3	–281 and –363
	−384 ± 3	−383 ± 2	−388−−400

Fig. 8. *Left*: Multi-component CaII K&H profiles in the spectrum of HD 190073. Right: The table from [14] presenting velocities of all local wind components observed in the CaII K&H doublet in the spectrum of HD 190073 from 1943 to 2000.

type: AB Aur, HD 36112, HD 31648 and others. Interpretation of such variability is shown in Fig. 7 (right). This is an example of model calculations of the profiles forming in the wind containing a rotating stream at different phases of its rotation. We used the Sobolev's approximation for moving media for calculations of source functions and optical thicknesses and exact numerical integration for profile construction. We can see that when the rotating outflowing stream moves near the line of sight (phase Φ from 3 to 11) the standing waves on the residuals are observed, and when it is far from the line of sight (Φ from 12 to 24) - the waves are running. The parameters of this particular model are presented in [13]. This type of variability speaks in favour of azimuthal inhomogeneity of the wind zones of Herbig Ae/Be stars.

5. UNIQUE HERBIG A2E–B8E STAR HD 190073

In this section we'd like to concentrate our attention on a very unusual Herbig Ae star HD 190073. About 50 spectra of the object were obtained during 9 years at 3 observatories [14]. The most striking peculiarity of the object is the blue-shifted absorption components of the resonance doublet of ionized calcium (Fig. 8, left). These lines are forming in the wind. Their profiles demonstrate a complex multi-component structure, they contain a lot of local lines. Different components of the profiles are collected in several separate groups. It is wonderful that velocities of the local features remain invariant during tens of years (Table in Fig 8, right). Later we carried out new spectroscopic observations at the Crimean AO. 180 high-resolution spectra near the $H\alpha$ line and DNaI doublet have been

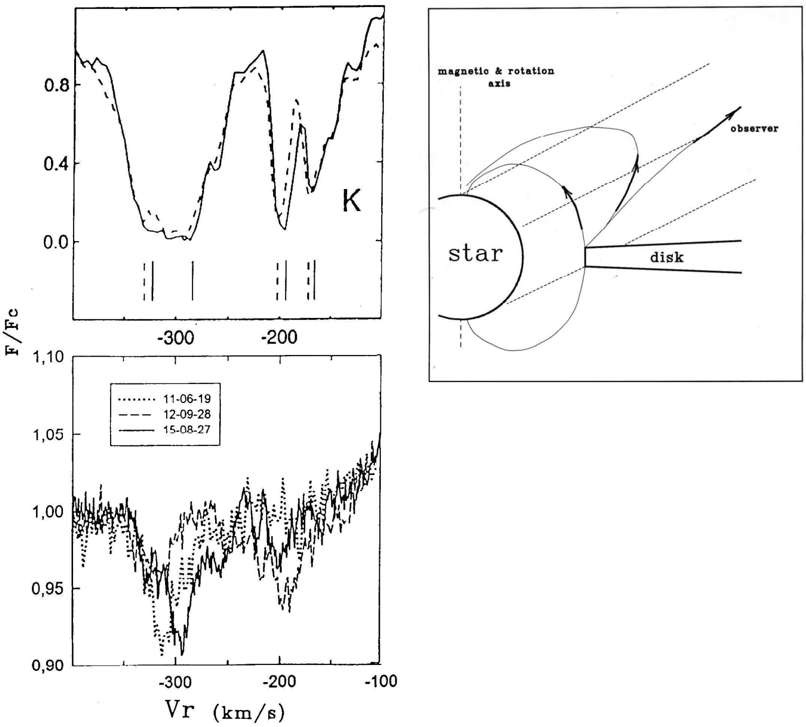

Fig. 9. Left: Comparison of the structure of the multi-component wind profiles of the CaII K&H doublet and of the NaD2 profile in the spectrum of HD 190073. Right: Illustration of a possible influence of the magnetic field configuration in the region of the disk/magnetosphere interaction on a velocity stratification of outflowing streams connected with a stratification of their directions relative to observer.

obtained from 2009 to 2018 [15]. The analysis of the data has shown that these lines also demonstrate multi-component profiles. But, in contrast to the calcium lines, the positions of individual components are variable in time. Nevertheless, they concentrate in the same several groups as the calcium lines (Fig. 9, left). This phenomenon remains unclear up to now. Hypothetically, we connected it with a specific configuration of the global magnetic field of the object. Fig. 9 (right) illustrates a possible influence of magnetic field configuration on the observed velocity stratification of outflowing streams connected with a stratification of their directions relative to the observer. The figure is taken from a paper by Camenzind [16]. But it still remains unclear: a) what is a real nature of such stratification, and b) why local wind components are more stable in the resonance CaII lines than in the resonance DNaI lines and in the $H\alpha$ line.

REFERENCES

1. Thé P.S., de Winter D., Perez M.R., 1994, A&AS, **104**, 315

2. Herbig G.H., 1960, ApJS, **4**, 337

3. Finkenzeller U. & Mundt R., 1984, A&AS, **55**, 109

4. Beskrovnaya N.G., Pogodin M.A., Shcherbakov A.G., Tarasov A.E., 1994, A&A, **287**, 564

5. Pogodin M.A., Miroshnichenko A.S., Bjorkman K.S., et al., 2000, A&A, **359**, 299

6. Pogodin M.A., Miroshnichenko A.S., Tarasov A.E.., et al., 2004, A&A, **417**, 715

7. Miroshnichenko A.S., Mulliss C.L., Bjorkman K.S., et al., 1998, PASP, **110**, 883

8. Alecian E., Catala C., Wade G.A., et al., 2008, MNRAS, **385**, 391

9. Bisyarina A.P., Sobolev A.M., Gorda S.Yu., et al., 2015, Astr.Bull., **70**, 299

10. Tjin A Djie H.R.E., van den Ancker M.E., Blondel P.F.C., et al., 2001, MNRAS, **325**, 1441

11. Pogodin M.A., Malanushenko V.P., Kozlova O.V., et al., 2006, A&A, **452**, 551

12. Pogodin M.A., 1994, A&A, **282**, 141

13. Pogodin M.A., Kozlova O.V., Alekseev I.Yu., et al., 2019, Astrophysics, **62**, 18

14. Pogodin M.A., Franco G.A.P., Lopes D.F., 2005, A&A, **438**, 239

15. Kozlova O.V., Pogodin M.A., Alekseev I.Yu., Dombrovskaya M.I., 2019, Astrophysics, **62**, 218

16. Camenzind M., Reviews in Modern Astronomy, 1990, **3**, 234

17. Corporon P. & Lagrange A.-M., A&AS, 1999, **136**, 429

18. Beskrovnaya N.G., Pogodin M.A., Najdenov I.D., et al., 1995, A&A, **298**, 585

19. Beskrovnaya N.G., Pogodin M.A., Miroshnichenko A.S., et al., 1999, A&A, **343**, 163

20. Beskrovnaya N.G., Pogodin M.A., 2004, A&A, **414**, 955